





Article

Itaconic Anhydride as a Bio-Based Compatibilizer for a Tung Oil-Based Thermosetting Resin Reinforced with Sand and Algae Biomass

Julio Antonio Conti Silva ^{1,2} , Seth Dever ², Anthony Siccardi ³, Drew Snelling ⁴, Ibrahim Al Qabani ⁵, Scott Thompson ⁵, Karin Goldberg ⁶ , Genevieve Baudoin ⁷, Talita Martins Lacerda ¹  and Rafael Lopes Quirino ^{2,*} 

¹ Department of Biotechnology, Universidade de São Paulo, Lorena 12602-810, SP, Brazil; julioconti@usp.br (J.A.C.S.); talitalacerda@usp.br (T.M.L.)

² Chemistry Department, Georgia Southern University, Statesboro, GA 30460, USA; sd06042@georgiasouthern.edu

³ Department of Biology, Georgia Southern University, Statesboro, GA 30460, USA; asiccardi@georgiasouthern.edu

⁴ Department of Manufacturing Engineering, Georgia Southern University, Statesboro, GA 30460, USA; dsnelling@georgiasouthern.edu

⁵ Department of Mechanical and Nuclear Engineering, Kansas State University, Manhattan, KS 66506, USA; alqabani@ksu.edu (I.A.Q.); smthompson@ksu.edu (S.T.)

⁶ Department of Geology, Kansas State University, Manhattan, KS 66506, USA; kgoldberg@ksu.edu

⁷ College of Architecture, Planning and Design, Kansas State University, Manhattan, KS 66506, USA; gbaudoin@ksu.edu

* Correspondence: rquirino@georgiasouthern.edu



Citation: Silva, J.A.C.; Dever, S.; Siccardi, A.; Snelling, D.; Al Qabani, I.; Thompson, S.; Goldberg, K.; Baudoin, G.; Martins Lacerda, T.; Quirino, R.L. Itaconic Anhydride as a Bio-Based Compatibilizer for a Tung Oil-Based Thermosetting Resin Reinforced with Sand and Algae Biomass. *Coatings* **2023**, *13*, 1188. <https://doi.org/10.3390/coatings13071188>

Academic Editor: Ioannis Pashalidis

Received: 2 June 2023

Revised: 28 June 2023

Accepted: 30 June 2023

Published: 1 July 2023



Copyright: © 2023 by the authors. Licensee MDPI, Basel, Switzerland. This article is an open access article distributed under the terms and conditions of the Creative Commons Attribution (CC BY) license (<https://creativecommons.org/licenses/by/4.0/>).

Abstract: In this work, renewable composites were prepared by the association of a thermosetting resin synthesized via free-radical polymerization, using a mixture of tung oil, *n*-butyl methacrylate, and divinylbenzene, with silica-rich fillers, namely an algae biomass with high silica content, and a well-sorted sand. Furthermore, to investigate if the interaction between the non-polar resin and polar reinforcements could be improved, enhancing the materials' mechanical properties, itaconic anhydride, a bio-derived molecule obtained from itaconic acid, was introduced to the resin composition. Thermogravimetric analysis (TGA) suggested that the thermal stability of the composites was overall not changed with the addition of itaconic anhydride. The mechanical properties of the sand composites, however, did improve, as the storage modulus at room temperature, measured by dynamic mechanical analysis (DMA), almost doubled in the presence of itaconic anhydride. The glass transition temperatures of the materials increased by approximately 30 °C when sand was used as a reinforcement. Water absorption experiments validated an increase in the polarity of the unreinforced resin by the addition of itaconic anhydride to its formulation. The composites, however, did not exhibit a significant difference in polarity in the presence of itaconic anhydride. Finally, scanning electron microscopy (SEM), equipped with energy dispersive spectroscopy (EDS), demonstrated better matrix–filler adhesion in the presence of itaconic anhydride for high-silica algae composites.

Keywords: tung oil; silica; algal biomass; itaconic anhydride; bio-based composites

1. Introduction

Polymers have become essential materials for humankind since synthetic macromolecules started to be produced and commercialized, being applied as thermoplastics, coatings, adhesives, fibers, etc. However, since the main sources for their synthesis are petroleum-based molecules, the search for alternative raw materials has intensified over the last few decades in order to reduce environmental problems. In this context, polysaccharides, terpenes, furans, and vegetable oils can be used to produce bio-based polymers.

It is important to mention, nevertheless, that the utilization of renewable resources for the production of polymers does not imply that the final product will be biodegradable [1,2].

The wide availability, low cost, and unique triglyceride structure of vegetable oils make them ideal candidates for polymer synthesis, since they can undergo direct polymerization or modification reactions, e.g., acrylation, epoxidation, and Diels–Alder reactions, producing monomers that are able to originate from linear to highly crosslinked materials [3,4]. Some recent studies report the production of bio-based monomers and polymers derived from vegetable oils [5–10]. Tung oil, for example, is very versatile from a chemical point of view. Its highly unsaturated structure, with approximately 80%–85% of α -eleostearic acid, a fatty acid chain containing three conjugated carbon-carbon double bonds, makes it very reactive to free-radical and cationic polymerizations [11].

Although benign from an environmental perspective and exhibiting promising thermal-mechanical properties, vegetable oil-based polymers usually need to be reinforced in order to compete with traditional petroleum-based materials used in structural applications. Several recent works describe the production of vegetable oil-based matrices reinforced with organic and inorganic fillers, such as lignocellulosic biomass [12–16], animal fibers [17], glass fibers [18], carbon nanotubes [19,20], carbon fibers [21], salts, and oxides [22].

Silicon dioxide (SiO_2), commonly known as silica, is found in nature mostly as a crystalline, well-defined network of Si and O atoms. The Si-O bond itself is polar due to the electronegativity difference between the atoms; however, in crystalline silica, the silicon atom is bonded to four other oxygen atoms in a tetrahedral arrangement, which makes the net dipole moment across the material equal to zero. The surface, on the other hand, is covered by silanol groups (Si-OH), granting some polarity to the material [23]. Silica is a promising reinforcement for composites. It improves the mechanical properties of soybean oil-based waterborne polyurethane [24], unsaturated epoxy and polyester resins [23,25], and polystyrene [26]. Silica is the major component of sand, which was used as a reinforcing agent for polymer matrices [27,28]. SiO_2 is also present in ash from algae biomass [29]. By acting as a functional reinforcement, algae biomass has been shown to improve the mechanical, electrical, and thermal properties of composites, while also having the advantage of being environmentally friendly, promoting the valorization of lignocellulosic biomass [30,31]. Despite the promising data reported, no detailed mechanism has been proposed for the specific enhancements observed when algae is used as reinforcement in composites. To the best of the authors' knowledge, no previous investigation has reported the synthesis of vegetable oil-based matrices reinforced with sand.

Another promising bio-based platform with great potential for the polymer industry is itaconic acid, an unsaturated dicarboxylic acid that can be produced by the microbial fermentation of fungi. Recently, itaconic acid has been used as a crosslinker for epoxidized vegetable oils, generating fully bio-based, reprocessable, thermosetting resins [32]. Developing relevant new applications, e.g., composites, for itaconic acid and its derivatives encourages improvements in the production of itaconic acid in biorefineries.

During the synthesis of composites, it is important to ensure that the matrix and the reinforcement have a good interaction with each other. Vegetable oil-based matrices are hydrophobic because of the long non-polar fatty acid chains. As a result, it does not interact well with hydrophilic reinforcements, such as lignocellulosic biomass or silica. Hence, a molecule that can interact with both hydrophobic and hydrophilic moieties may be employed to promote improved compatibility between the phases of the composite. In the recent past, several compatibilizer agents were used to improve the interaction between vegetable oil-based matrices and hydrophilic fillers, such as fatty acids [33], asolectin [34], and maleic anhydride [35]. In this context, itaconic anhydride (ITA), an itaconic acid derivative, is a promising replacement for maleic anhydride, since they share a very similar chemical structure, with ITA having the advantage of being bio-based. Its carbon-carbon double bond allows its free-radical polymerization, and consequently, it can be incorporated into a vegetable oil-based resin as a comonomer. The hydroxyl groups of the reinforcements can then open the anhydride group present in the resin, favoring

their interaction and therefore leading to a composite with enhanced mechanical properties. Recently, it has been determined that the addition of ITA to a tung oil-based thermosetting resin matrix reinforced with *Miscanthus*, pine wood, or algal biomass indeed increased their thermal-mechanical properties, confirming its role as a compatibilizer [36].

In this work, composites made of tung oil, divinylbenzene (DVB), and *n*-butyl methacrylate (BMA), reinforced with either sand or high-silica algae biomass, are reported. In order to improve the interaction between the non-polar resin and the polar reinforcements, itaconic anhydride (ITA) was investigated as a compatibilizer agent. The thermal-mechanical properties were assessed by thermogravimetric analysis (TGA), differential scanning calorimetry (DSC), and dynamic mechanical analysis (DMA). The morphology of the composites was investigated via scanning electron microscopy (SEM) and energy dispersive X-ray spectroscopy (EDS).

2. Experimental

2.1. Materials

Tung oil (80% ester of eleostearic acid; 20% ester of linolenic, 9,12-linoleic, oleic, stearic, and palmitic acids) and di-*tert*-butyl peroxide (DTBP) (98%) were acquired from Sigma-Aldrich (St. Louis, MO, USA), divinylbenzene (DVB) (80%, mixture of isomers) was purchased from Alfa Aesar (Ward Hill, MA, USA), *n*-butyl methacrylate (BMA) (99%) was obtained from Acros Organics (Morris Plains, NJ, USA), and itaconic anhydride (ITA) (95%) was purchased from TCI America (Portland, OR, USA). All chemicals were used as received. The sand sample was collected in northeastern Kansas at the Buffalo Track Canyon Nature Trail, Kanopolis Lake State Park (Marquette, KS, USA), Ellsworth (38.6737192, −97.9997259) as a fine-to-medium-sized, well-sorted, dominantly quartzose sediment (Figure 1). The average sediment size was measured to be approximately 250 μm . No grain-size separation was performed on this sample.

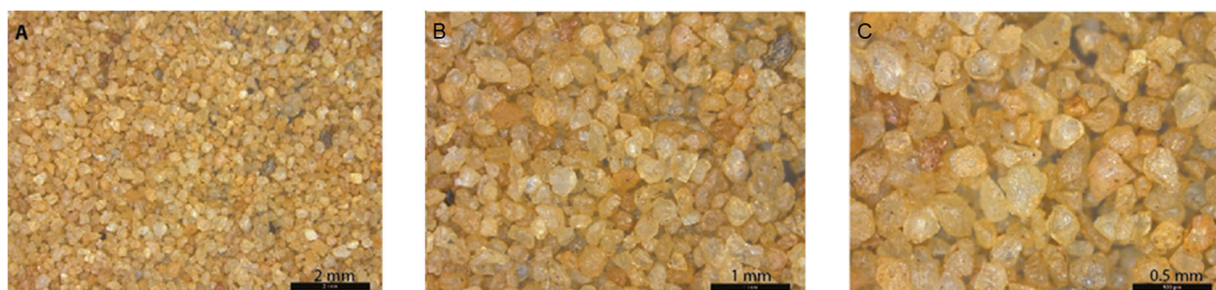


Figure 1. Photographs of the sand sample collected in KS, formed over the Cretaceous Dakota Formation. Photographs display the sediments (A) without any magnification, (B) 2 \times magnification, and (C) 4 \times magnification.

2.2. Methods

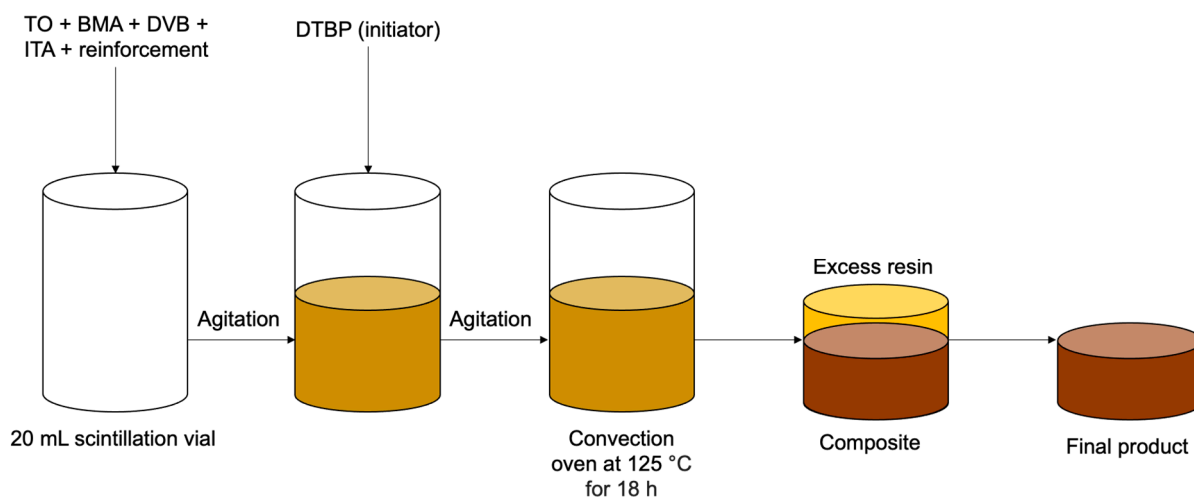
2.2.1. Algal Biomass

Algal biomass was collected from experimental algal turf scrubbers (ATS) located at Priest Landing, Savannah, GA, USA. Three, four-lane (1 foot wide/lane, 30 feet long) ATS systems were utilized to examine the effects of different substrates (2-D, advanced 3-D) and matrix compositions (polyethylene, polypropylene). A control (no mesh) lane was included in each system. Each lane on the ATS system was randomly assigned and outfitted with a mesh substrate (i.e., treatment) or designated as a control. Raw brackish water was pumped from the Skidaway River at a rate of approximately 189 L/min with a dump bucket pulse rate of approximately 20 s. On a weekly basis, biomass was scraped from each lane using a squeegee. Water flow was halted on the system for the duration of harvests (~1.5 h). A felt-lined fish harvest basket was placed at the end of each lane where biomass was collected. Biomass was allowed to de-water in the felt-lined fish harvest basket for approximately six hours prior to being frozen for later use. The high-silica algae

biomass was thawed, dried at 70 °C for 24 h under vacuum, ground, and sieved. Three different particle sizes were utilized in this study, namely 425–850 µm, 150–425 µm, and <150 µm.

2.2.2. Preparation of Tung Oil-Based Composites

Two different resin formulations were used, i.e., with or without ITA. The former was composed of 40 wt.% of tung oil, 30 wt.% of BMA, 20 wt.% of DVB, and 10 wt.% of ITA, while the latter used 50 wt.% of tung oil, 30 wt.% of BMA, and 20 wt.% of DVB. The resin components were added to a 20 mL scintillation vial and thoroughly mixed before the addition of the reinforcement. For the resin that contained ITA, the mixture was heated until the ITA was completely melted. The reinforcement was weighed, added to the resin mixture, and the contents of the vial were thoroughly agitated. Then, an additional 5 wt.% (with respect to the total weight of the resin) of the initiator DTBP was added to the mixture. The contents of the vial were thoroughly mixed one last time before being cured at 125 °C for 18 h. After curing, a thin layer of unreinforced resin could be observed on top of the composites (Scheme 1). This layer was cut off, and the composites were weighed again to determine the actual reinforcement load, which was approximately 83 wt.% for sand, and approximately 52 wt.% for high-silica algae. Table 1 summarizes all compositions prepared in this work, indicating the reinforcement used and whether the sample contained ITA or not.



Scheme 1. Schematic representation of composite preparation.

Table 1. Summary of all samples prepared.

| Reinforcement | Sample Name | Reinforcement Particle Size | ITA wt. % |
|-------------------|--------------|-----------------------------|-----------|
| - ^a | TO Resin | - | - |
| - ^a | TO Resin ITA | - | 10 |
| Sand | S | <500 µm | - |
| Sand | S ITA | <500 µm | 10 |
| High-silica algae | HSA 850 | 425–850 µm | - |
| High-silica algae | HSA 425 | 150–425 µm | - |
| High-silica algae | HSA 150 | <150 µm | - |
| High-silica algae | HSA 150 ITA | <150 µm | 10 |

^a Unreinforced samples were previously prepared and characterized as reported in the literature [3,5].

2.2.3. Characterization

A Q20 DSC instrument (TA Instruments, New Castle, DE, USA) was used to perform DSC experiments. For each test, approximately 10 mg of the samples were sealed in aluminum hermetic pans and then heated from −20 °C to 150 °C, at a heating rate of 10 °C/min under an N₂ atmosphere. TGA tests were conducted on a Q50 TGA instrument

(TA Instruments, New Castle, DE, USA) under an air atmosphere. Approximately 10 mg of the samples were heated in platinum pans from room temperature to 650 °C at a rate of 10 °C/min, and the weight loss was measured as a function of temperature.

DMA experiments were conducted on a Q800 DMA instrument (TA Instruments, New Castle, DE, USA) with a 3-point bend fixture. The experiments were carried out at a frequency of 1 Hz and an amplitude of 14 µm. The samples were cut into specimens with approximate dimensions of 22.0 mm × 10.0 mm × 2.0 mm (length × width × thickness, respectively). Each specimen was cooled to −60 °C and then heated to 150 °C at a heating rate of 3 °C/min under an iso-strain mode. Each sample was run at least three times, and the results shown here represent the average of the trials.

Water absorption experiments were carried out in triplicate in order to determine the materials' ability to absorb water. The samples were cut and weighed at their dry state (W_d) prior to their submersion in 5 mL of water for 24 h. Then, the samples were dried with kimwipes to remove the excess water and weighed at their wet state (W_w). The water absorption percentage was then calculated by Equation (1). The statistical significance of the DMA and water uptake results was assessed by one-way analysis of variance (ANOVA), and Tukey's honestly significant difference (HSD) test was carried out in order to determine which means were significantly different from each other. The significance level considered for all the analyses was 5%.

$$\text{Water absorption (\%)} = 100 \times \frac{w_w - w_d}{w_d} \quad (1)$$

Infrared spectroscopy was executed on a Thermo Nicolet iS10 FTIR spectrometer (Thermo Scientific, Waltham, MA, USA) with an attenuated total reflectance (ATR) accessory. The spectra were collected in the 400–4000 cm^{−1} spectral region, with 32 scans, and 4 cm^{−1} resolution.

SEM images of the cross-section of each composite were obtained in a JSM-7600F Field Emission Scanning Electron Microscope (JEOL, Peabody, MA, USA), using an acceleration voltage of 3.0 kV for composites reinforced with sand and 5.0 kV for the ones reinforced with algae biomass. Secondary electron imaging mode (SEI) and an emission current of approximately 81 µA were used. The samples were previously sputter-coated with gold using a Desk V coating system (Denton Vacuum, Moorestown, NJ, USA). The SEM was equipped with energy dispersive spectroscopy (EDS), which performed the elemental analysis of the composites. For this technique, an acceleration voltage of 20.0 kV was employed.

3. Results and Discussion

The thermal stability of the samples was assessed via TGA, and the thermograms are shown in Figure 2. Since the organic material of the resins was completely degraded at temperatures up to 650 °C, that was arbitrarily chosen as the final temperature of the tests. As previously reported, the presence of itaconic anhydride in the resin does not impact its thermal stability, resulting in overlapping thermal degradation profiles [36]. According to Figure 2A, high-silica algae biomass lost approximately 5% of its weight before 150 °C, most likely due to the evaporation of moisture. Algae biomass is a lignocellulosic material rich in hydroxyl groups (−OH), which are highly polar and able to interact with water through hydrogen bonding. Around 82 wt.% of pure high-silica algae biomass remained at the end of the run, indicating that the biomass indeed has a large amount of silica and other inorganic materials. High-silica algae composites barely lose moisture, having a weight loss of around 2% before 150 °C, while the residues after the analysis varied between 40 and 50 wt.%. Due to the presence of resin, the composites are more hydrophobic than the reinforcement alone, explaining the low moisture content observed in this analysis and the reduction in residue obtained after each run. After the evaporation of moisture, high-silica algae started to degrade at around 240 °C, whereas for unreinforced resins, the degradation started around 320 °C. Hence, even though the reinforcement contains a high content of

inorganic material, its organic content is less thermally stable than the resin alone. For this reason, the addition of resin improves the thermal stability of the fillers, as the composites started to degrade at around 270 °C. The different particle sizes (Figure 2A) affected the thermal stability of the high-silica algae composites. Usually, smaller particle sizes alone have a smaller temperature gradient between their outer and inner parts, which translates to them being thermally degraded at lower temperatures than larger particles [37]. However, smaller particle sizes have higher surface areas; consequently, the resin can interact better with the reinforcement, generating fewer voids inside the composite. Therefore, more energy is required to thermally degrade the material in comparison to composites made with larger particle sizes. Composite HSA 150 indeed exhibited the highest thermal stability of the three. HSA 850 was only slightly more stable than HSA 425 at lower temperatures, but it completely degraded faster, suggesting that the smaller particle sizes were indeed able to interact better with the matrix and improve the material's thermal stability. A similar trend was observed for poly(methyl methacrylate/silica nanocomposites [38]. The presence of ITA (Figure 2B) surprisingly rendered the composite slightly less thermally stable at lower temperatures. The presence of a compatibilizer promotes a better interaction between the matrix and filler and should, consequently, improve the material's thermal stability. A previous study showed that the addition of ITA indeed considerably improved the thermal stability of tung oil-based matrices reinforced with lignocellulosic biomass, due to the better interaction between continuous and disperse phases, leading to a higher demand for energy necessary to degrade the fillers [36]. In this case, however, the filler barely degraded because of its high inorganic content, even if the compatibility was sufficient. The degradation observed in these composites was dominated by the resin. Hence, since the presence of ITA does not affect the thermal stability of the resin, this could be an explanation for the overall trends observed in the TGA results.

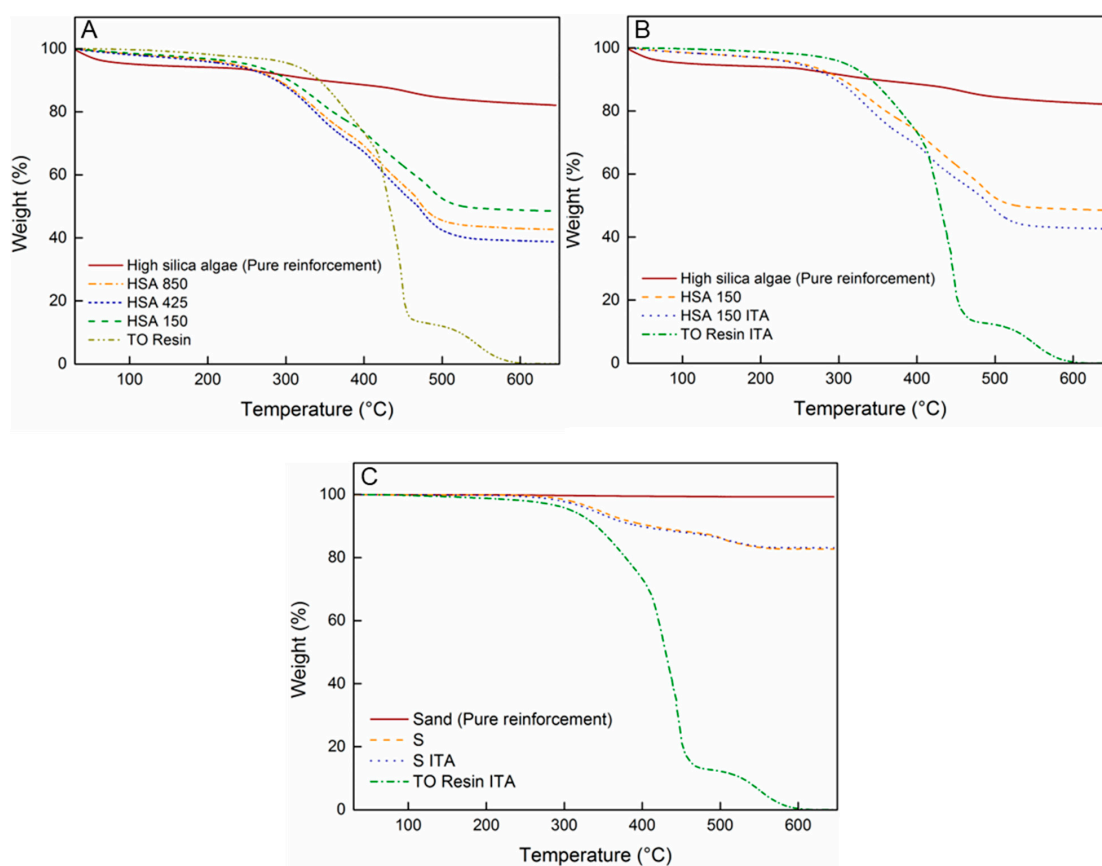


Figure 2. TGA curves of (A) high-silica algae composites with different particle sizes, (B) high-silica algae composites with and without ITA, and (C) sand composites with and without ITA.

Pure sand did not degrade at all (Figure 2C), presenting a single weight loss of 0.1% at 150 °C. Despite the presence of superficial silanol groups (Si-OH), the bulk of sand is non-polar, which explains the low content of moisture eliminated at 150 °C. The composites started to degrade at lower temperatures (290 °C) than the unreinforced resin (320 °C). Despite not degrading at this temperature, sand has a low specific heat, meaning that it needs a small amount of energy to increase its temperature. Thus, the composites might require a smaller amount of heat to increase their temperature compared to the unreinforced resin, consequently degrading faster. The addition of ITA did not seem to affect the thermal stability of the composites at all. Similar to the high-silica algae composites, this phenomenon could be a result of the non-degradation of sand.

DSC measurements were performed in order to determine whether the cure of the composites was complete or not, and the results are displayed in Figure 3. The presence of exothermic peaks at around 100–130 °C would indicate residual polymerization taking place during the analysis, indicating the incompleteness of the cure process. Since no exothermic peaks were observed in any of the DSC graphs (Figure 3), it can be concluded that residual polymerization was negligible or did not happen, meaning that most of the co-monomers fully polymerized during the curing process, leading to the conclusion that neither the reinforcement, its particle size, nor the presence of ITA negatively impact the curing process. The presence of endothermic peaks, however, indicates the elimination of volatiles and moisture. Neither the resins with no reinforcements nor the sand samples, and consequently the composites reinforced by them (Figure 3C), showed endothermic peaks. In accordance with the TGA, this result indicates that, despite the presence of polar Si-OH groups at the surface of the sand, the absorption of moisture from the air is not significant. The pure high-silica algae (Figure 3A,B), on the other hand, showed a prominent endothermic peak at approximately 135 °C, and all the composites made with high-silica-algae biomass exhibit a modest endothermic peak at 68–94 °C. Since the high-silica algae biomass was dried before being added to the composites, and considering that the polymerization happened at 125 °C, traces of moisture were probably removed. Therefore, the endothermic peak present in the DSC thermograms of the composites is possibly related to the moisture absorbed by the composites themselves, which is expected to be lower than the pure reinforcement because of the presence of the non-polar tung oil-based resin. This could explain the difference between the areas and the peak temperatures of the pure reinforcement and its composites.

The mechanical properties of the composites were assessed by DMA, and the main results are presented in Table 2 and Figure 4. Table 2 reports E' at room temperature (25 °C) and at the rubbery plateau ($T_g + 50$ °C). The T_g was determined by the tan delta peak (Figure 4B). It was not possible to obtain uniform DMA specimens for the high-silica algae composites due to the excessive presence of bubbles/air pockets in those samples.

Table 2. DMA results for tung oil-based resins without reinforcement, and sand composites with and without itaconic anhydride. The results presented correspond to the average of a minimum of three trials, unless otherwise noted.

| Sample | E' at 25 °C (MPa) | T_g (°C) | E' at $T_g + 50$ °C (MPa) |
|-------------------|---------------------|------------|-----------------------------|
| TO Resin [36] | 518 ± 108 | 26 ± 6 | 146 ± 52 |
| TO Resin ITA [36] | 232 ± 118 | 32 ± 5 | 26 ± 16 |
| S ^a | 479 ± 70 | 67 ± 1 | 134 ± 59 |
| S ITA | 922 ± 67 | 60 ± 6 | 219 ± 187 |

^a Only two repeats were possible with the sand composite in the absence of ITA due to premature failure of the sample.

As is the case for all polymerization reactions, it is not possible to ensure that all the monomers react simultaneously. This invariably creates a heterogeneous resin, which is translated into the DMA results. The high standard deviation values of some of the measurements reflect the heterogeneity of the material. Nevertheless, some trends can still be observed, and the one-way ANOVA indicated that there was a statistically significant

difference between at least two samples regarding the storage modulus at 25 °C and the glass transition temperatures (T_g) measured with DMA ($F = 27.9$, $p = 1.4 \times 10^{-4}$; and $F = 44.9$, $p = 6.1 \times 10^{-5}$, for E' at 25 °C and T_g , respectively). The results for the storage modulus at $T_g + 50$ °C, on the other hand, did not considerably differ between the samples tested ($F = 1.68$, $p = 0.26$).

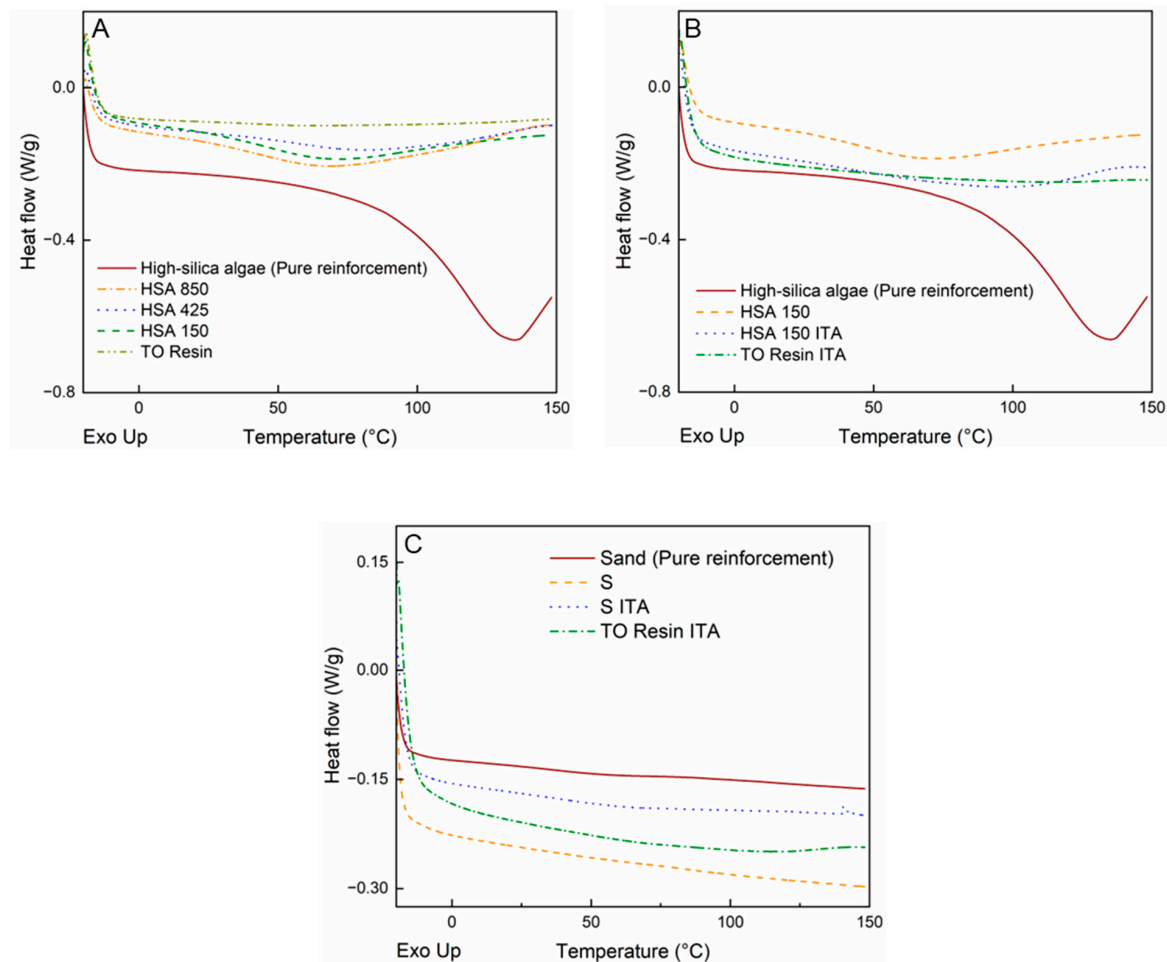


Figure 3. DSC curves of (A) high-silica algae with different particle sizes, (B) high-silica algae with and without ITA, and (C) sand composites with and without ITA.

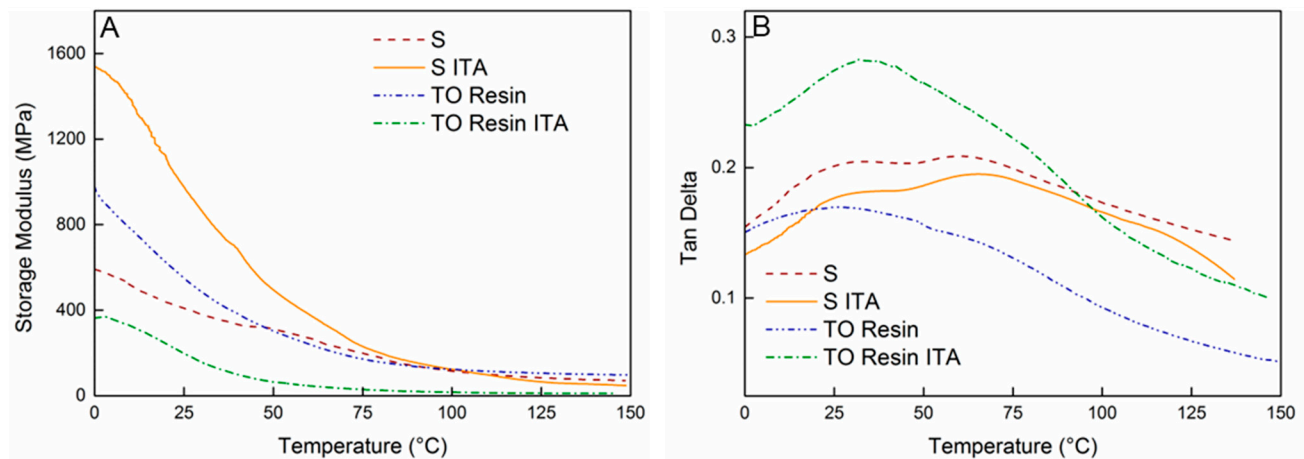


Figure 4. Representative DMA curves of composites reinforced with sand, and resins with no reinforcements, showing (A) storage modulus vs. temperature and (B) tan delta vs. temperature.

Tukey's HSD test confirmed that the addition of ITA affected the storage moduli at 25 °C in the case of unreinforced resins ($p = 0.024$). In fact, this effect was also observed when asolectin was added to the formulation of a tung oil-based resin due to the inferior amount of carbon–carbon double bonds in the structure of asolectin compared to tung oil, leading to a lower crosslink density [34]. The structure of ITA is indeed less unsaturated than tung oil. Consequently, the replacement of tung oil by ITA in the formulation of the resins led to a decrease in the crosslink density and, therefore, in the storage modulus. The T_g , however, did not significantly change with the addition of ITA to the resin ($p = 0.57$).

The reinforcement of the resin did not seem to have a significant positive effect on the storage modulus of the material at room temperature, considering the standard deviations and Tukey's HSD ($p = 0.95$). However, the addition of ITA almost doubled the storage modulus at room temperature of the composite. Samples S ITA and S were indeed statistically significantly different from each other ($p = 1.8 \times 10^{-3}$). This result is a strong indication that ITA is a good compatibilizer between the tung oil-based matrix and the sand reinforcement. It is believed that the interaction between the silanol groups from sand and the anhydride group from ITA promotes an enhanced interface interaction between them. Thus, the stress is better transferred from the matrix to the filler, resulting in higher storage moduli. This phenomenon was also observed between tung oil-based resins reinforced with other lignocellulosic biomass, such as maleic anhydride [35], asolectin [34], and itaconic anhydride [36].

The T_g was surprisingly affected by the addition of sand to the resin. Both sand-reinforced composites shared similar T_g s, with no significant difference between them according to Tukey's HSD test ($p = 0.54$). However, their T_g was considerably higher than that of the unreinforced resins, with an increase of approximately 30 °C ($p = 1.9 \times 10^{-4}$ for S vs. TO Resin, and $p = 7.8 \times 10^{-4}$ for S ITA vs. TO Resin ITA). The glass transition temperature is an intrinsic characteristic of semi-crystalline and amorphous polymers that can be affected by a series of factors. The addition of a reinforcement per se should not alter the T_g of the matrix unless there is a change in the polymerization process. Sand is a material with a low specific heat, meaning that it takes a small amount of energy to increase its temperature, and a low heat transfer coefficient, implying that it can retain heat for longer periods of time. During the curing process, these properties of sand could have impacted the polymerization of the resin, leading to a material with different polymer chains compared to the pure resins, and, therefore, a different glass transition temperature.

Even though the averages of E' at $T_g + 50$ °C are not significantly different, the trends suggest that TO Resin ITA has the lowest values amongst the samples, which can also be due to the lower crosslink density resulting from the replacement of tung oil (~9 carbon–carbon double bonds per triglyceride) with the less unsaturated ITA (one carbon–carbon double bond per molecule). As expected, S ITA exhibits the highest storage modulus at room temperature and at $T_g + 50$ °C. However, it is worth noting that the values obtained for E' at $T_g + 50$ °C are not statistically different from the other composites.

Water absorption tests were performed to give an insight into the effect of ITA and reinforcements on the polarity of the composites. Water absorption results are presented in Table 3. One-way ANOVA confirmed that there were at least two averages that were significantly different from each other ($F = 21.3$, $p = 1.4 \times 10^{-5}$). As expected, the resins without reinforcement showed the lowest percentages of water absorption, which is a result of the highly non-polar components present in their formulation. The presence of ITA significantly increased the water absorption percentage of the resin (Tukey's HSD p -value: 0.027). This is an outcome of the replacement of tung oil by ITA. The polar anhydride group present in TO Resin ITA can interact with water via dipole–dipole interactions, resulting in greater water absorption.

The addition of lignocellulosic reinforcements to the tung oil-based resins considerably increased their water absorption. The addition of high-silica algae increased the water absorption 10-fold, whereas the sand increased it by six times ($p = 2.0 \times 10^{-5}$ for TO Resin vs. HSA 150, $p = 0.017$ for TO Resin vs. S, and $p = 5.8 \times 10^{-3}$ for HSA 150 vs. S). This

result is probably due to the presence of hydroxyl groups in the reinforcements, which allow the creation of hydrogen bonds between filler and water that are much stronger than ordinary dipole–dipole interactions. The difference between high-silica algae and sand is in accordance with the results found on TGA and DSC. Similar results were also obtained with other lignocellulosic biomass [36].

Table 3. Water absorption results of select samples.

| Sample | Water Absorption (wt.%) |
|-------------------|-------------------------|
| TO Resin [36] | 0.3 ± 0.3 |
| TO Resin ITA [36] | 1.7 ± 0.1 |
| HSA 150 | 3.5 ± 0.6 |
| HSA 150 ITA | 3.4 ± 0.2 |
| S | 1.8 ± 0.6 |
| S ITA | 1.9 ± 0.5 |

Surprisingly, the introduction of ITA in the composite formulation did not change the water absorption at all. The water absorption is based on the interaction of water with polar groups, e.g., -OH groups, present in the material. When ITA was not present in the composite, the resin and the reinforcement probably did not mix well (Figure 5A), and the -OH groups present in the filler were free to interact with water during the water absorption experiment. When ITA is present, the -OH groups from the fillers react with the anhydride group, opening the five-membered ring, and originating a carboxylic acid (Figure 5B), which is able to interact with water. Therefore, despite the addition of ITA and its interaction with the reinforcement, the net number of -OH groups is the same in both instances, resulting in similar water absorption results. Figure 5 is an illustration of the reaction believed to take place between the compatibilizer and the reinforcement. It illustrates that, regardless of the presence of ITA, the net number of hydroxyl groups is still the same, which explains why the water absorption did not change.

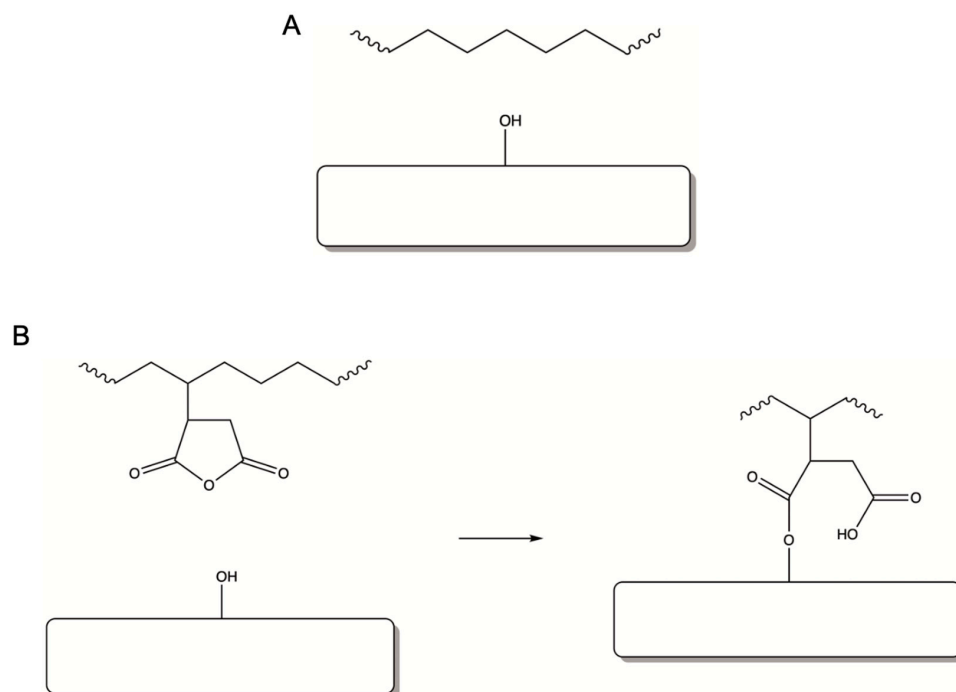


Figure 5. Schematic representation of (A) composite in the absence of ITA, evidencing the presence of -OH groups on the reinforcement, and (B) composite in the presence of ITA, showing the interaction between the -OH and anhydride groups.

To better investigate the assumption that ITA and -OH groups interacted in the composites, FTIR spectroscopy was performed, and spectra are shown in Figure 6. High-silica algae presented a band centered around 3430 cm^{-1} associated with hydroxyl groups. These bands also appeared in both composites with and without ITA. For sand, however, the OH band is barely noticeable, which is in accordance with TGA and DSC results, in which sand did not absorb considerable moisture. Pure itaconic anhydride presented two C=O stretching bands characteristic of cyclic anhydrides [39], a symmetric one at 1843 cm^{-1} , and an asymmetric one at 1764 cm^{-1} . The composites containing ITA did not exhibit the symmetric C=O stretching band at 1843 cm^{-1} , which gives a strong indication that the anhydride ring was indeed opened during the polymerization of the composites, and the only difference between the composites with and without ITA was the appearance of a band at 1780 cm^{-1} in the former's spectrum, which is probably a shift of the band at 1764 cm^{-1} due to the opening of the ring, originating a new ester and a carboxylic acid. All the composites exhibited a band at 1720 cm^{-1} , likely corresponding to C=O stretching vibrations of ester, present in tung oil and butyl methacrylate, co-monomers of the resins. Overall, FTIR gave indications of the reaction between the OH groups present in the reinforcements and the anhydride ring.

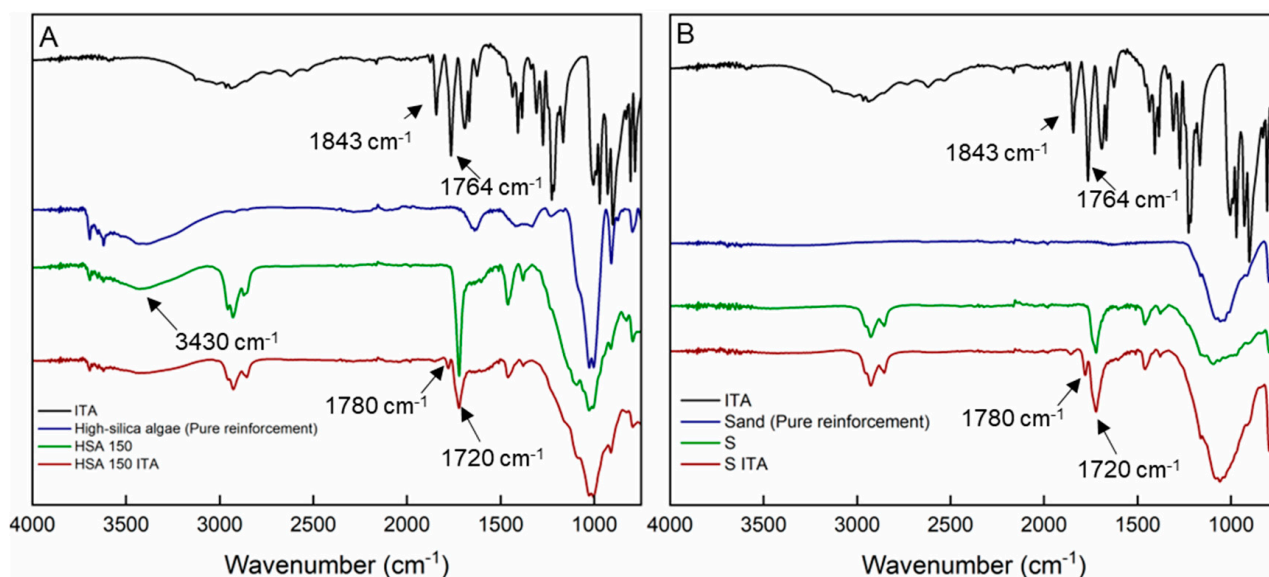


Figure 6. FTIR spectra of (A) ITA, high-silica algae and its composites, and (B) ITA, sand and its composites.

The morphology of the materials was assessed via SEM, while EDS mapping was performed to help distinguish matrix and reinforcement on the images (Figure 7). The reinforcements correspond to the silicon and oxygen-rich regions (blue and green, respectively), whereas carbon-rich regions (magenta) correspond to the matrix. The addition of ITA to the composites reinforced with high-silica algae evoked some microscopic divergences. In the absence of ITA (Figure 7A,B), the interface between matrix and reinforcement exhibits noticeable fissures, indicating that there is poor interaction between the two components of the composite. In the presence of ITA (Figure 7C,D), on the other hand, the gaps are not noticeable, and the matrix and reinforcement are indistinguishable without the elemental mapping. This strongly supports the idea that ITA did, in fact, promote a better interaction between the non-polar tung oil-based resin and the polar high-silica algae biomass. The composites reinforced with sand, however, presented no significant microscopic discrepancy between samples in the absence (Figure 7E,F) or presence (Figure 7G,H) of ITA. Both samples look virtually identical under the microscope, and the interface between sand and resin appears to be well established in both cases.

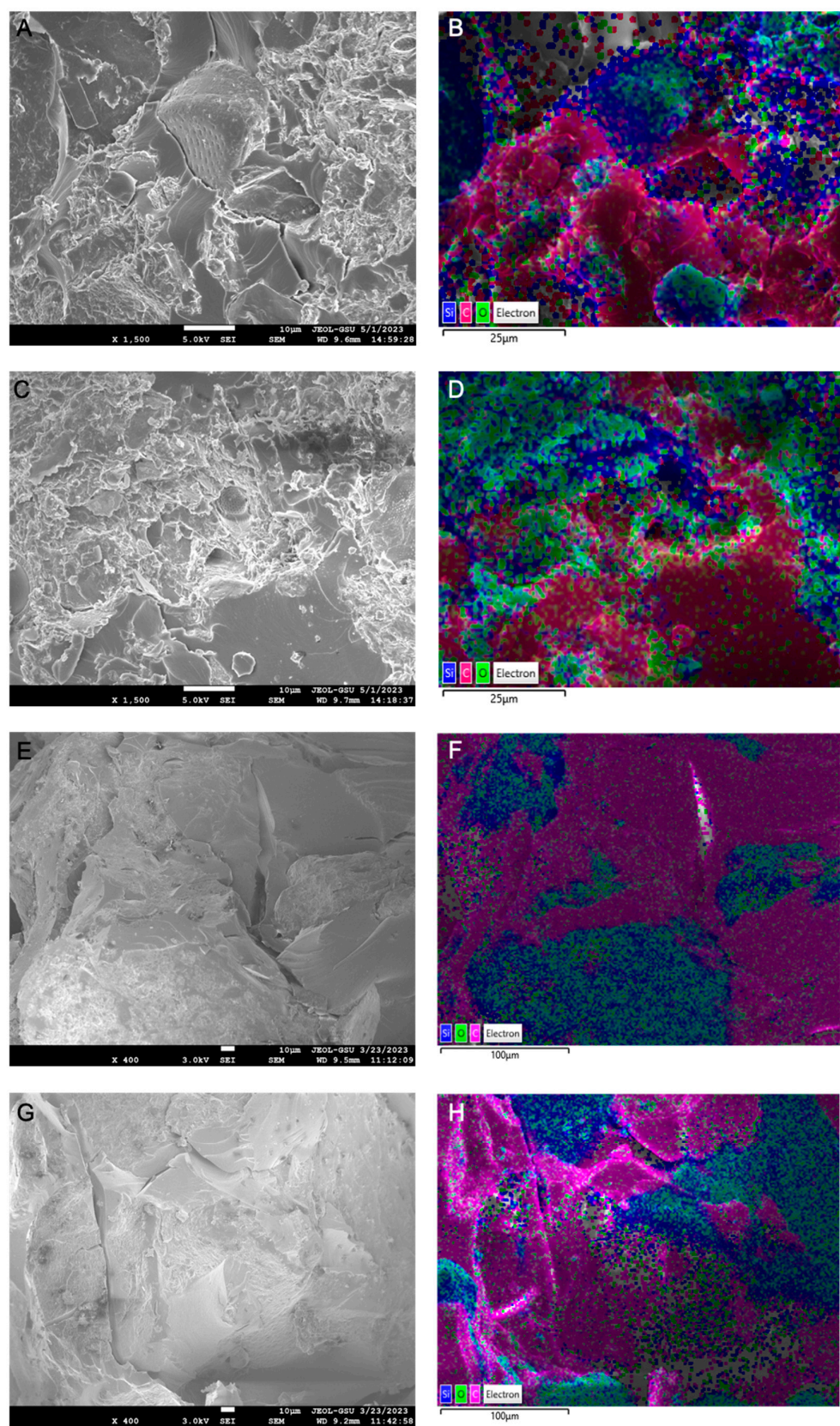


Figure 7. SEM images (left) and respective elemental mapping by EDS (right) of samples (A,B) HSA 150, (C,D) HSA 150 ITA, (E,F) S, and (G,H) S ITA. Silicon, oxygen, and carbon are shown in blue, green, and magenta, respectively.

4. Conclusions

In this work, composites made from a tung oil/divinylbenzene/butyl methacrylate resin reinforced with either 52 wt.% of high-silica algae biomass or 83 wt.% of a well-sorted, fine to medium sand were produced. Thermal analyses showed that neither the type of reinforcement, its particle size, nor the presence of ITA negatively impacted the curing process, and that the addition of ITA did not impact the thermal stability of the composites. The presence of ITA considerably increased the storage modulus of the sand composites at room temperature and the water absorption of the unreinforced resins, but not the composites. The ring-opening of ITA by the hydroxyl groups from the reinforcements was supported by FTIR. Finally, SEM images indicated that ITA developed effective matrix-reinforcement compatibility in high-silica algae composites, but no changes were observed for sand composites. The results indicate that, although it was not possible to identify any microscopic effect of the addition of ITA to sand composites, the enhancement of the mechanical properties suggests that the inclusion of itaconic anhydride as a co-monomer in a tung oil-based resin increases the polymer polarity and improves the interaction between matrix and reinforcement. Although DMA was not possible for high-silica algae-based composites, the results that were obtained were also encouraging.

Author Contributions: Conceptualization, D.S., G.B. and R.L.Q.; methodology, J.A.C.S. and S.D.; software, I.A.Q. and K.G.; validation, R.L.Q. and S.T.; formal analysis, J.A.C.S.; investigation, J.A.C.S.; resources, A.S. and K.G.; data curation, J.A.C.S.; writing—original draft preparation, J.A.C.S.; writing—review and editing, R.L.Q.; visualization, J.A.C.S.; supervision, R.L.Q.; project administration, R.L.Q. and S.T.; funding acquisition, T.M.L. and S.T. All authors have read and agreed to the published version of the manuscript.

Funding: This research was funded by Coordenação de Aperfeiçoamento de Pessoal de Nível Superior-Brasil (CAPES)–Finance Code 001, the National Science Foundation (Award #2229267), and FAPESP (São Paulo Research Foundation, Grant 2022/12451-6). The APC was graciously waived for this publication.

Informed Consent Statement: Not applicable.

Data Availability Statement: All relevant data related to this study is included in this manuscript.

Conflicts of Interest: The authors declare no conflict of interest.

References

1. Rosenboom, J.-G.; Langer, R.; Traverso, G. Bioplastics for a Circular Economy. *Nat. Rev. Mater.* **2022**, *7*, 117–137. [\[CrossRef\]](#)
2. Gandini, A.; Lacerda, M.; Monomers, T. Macromolecular Materials from Renewable Resources: State of the Art and Perspectives. *Molecules* **2021**, *27*, 159. [\[CrossRef\]](#) [\[PubMed\]](#)
3. Tremblay-Parrado, K.-K.; García-Astrain, C.; Avérous, L. Click Chemistry for the Synthesis of Biobased Polymers and Networks Derived from Vegetable Oils. *Green Chem.* **2021**, *23*, 4296–4327. [\[CrossRef\]](#)
4. Silva, J.A.C.; Grilo, L.M.; Gandini, A.; Lacerda, T.M. The Prospering of Macromolecular Materials Based on Plant Oils within the Blooming Field of Polymers from Renewable Resources. *Polymers* **2021**, *13*, 1722. [\[CrossRef\]](#)
5. Gomez, J.C.; Zakaria, R.; Aung, M.M.; Mokhtar, M.N.; Yunus, R. Synthesis and Characterization of Polyurethanes from Residual Palm Oil with High Poly-Unsaturated Fatty Acid Oils as Additive. *Polymers* **2021**, *13*, 4214. [\[CrossRef\]](#)
6. Grauzeliene, S.; Navaruckiene, A.; Skliutas, E.; Malinauskas, M.; Serra, A.; Ostrauskaite, J. Vegetable Oil-Based Thiol-Ene/Thiol-Epoxy Resins for Laser Direct Writing 3D Micro-/Nano-Lithography. *Polymers* **2021**, *13*, 872. [\[CrossRef\]](#)
7. Abbasi, A.; Yahya, W.Z.N.; Nasef, M.M.; Moniruzzaman, M.; Ghumman, A.S.M. Copolymerization of Palm Oil with Sulfur Using Inverse Vulcanization to Boost the Palm Oil Industry. *Polym. Polym. Compos.* **2021**, *29*, S1446–S1456. [\[CrossRef\]](#)
8. Alarcon, R.T.; Gaglieri, C.; Lamb, K.J.; Cavalheiro, É.T.G.; North, M.; Bannach, G. A New Acrylated Monomer from Macaw Vegetable Oil That Polymerizes without External Photoinitiators. *J. Polym. Res.* **2021**, *28*, 425. [\[CrossRef\]](#)
9. Sain, S.; Åkesson, D.; Skrifvars, M. Synthesis and Properties of Thermosets from Tung Oil and Furfuryl Methacrylate. *Polymers* **2020**, *12*, 258. [\[CrossRef\]](#)
10. Anbinder, S.; Meiorin, C.; Macchi, C.; Mosiewicki, M.A.; Aranguren, M.I.; Somoza, A. Structural Properties of Vegetable Oil Thermosets: Effect of Crosslinkers, Modifiers and Oxidative Aging. *Eur. Polym. J.* **2020**, *124*, 109470. [\[CrossRef\]](#)
11. Sharma, V.; Kundu, P.P. Addition Polymers from Natural Oils—A Review. *Prog. Polym. Sci.* **2006**, *31*, 983–1008. [\[CrossRef\]](#)

12. Todorovic, A.; Blößl, Y.; Oreski, G.; Resch-Fauster, K. High-Performance Composite with 100% Bio-Based Carbon Content Produced from Epoxidized Linseed Oil, Citric Acid and Flax Fiber Reinforcement. *Compos. Part A Appl. Sci. Manuf.* **2022**, *152*, 106666. [\[CrossRef\]](#)
13. Seabra, C.P.; Sousa, A.C.; Bragança, I.M.F.; Silva, C.M.A.; Robalo, M.P.; Loja, M.A.R.; Martins, P.A.F. On the Performance and Recyclability of a Green Composite Based on AESO Resin. *J. Manuf. Mater. Process.* **2020**, *4*, 65. [\[CrossRef\]](#)
14. Sain, S.; Åkesson, D.; Skrifvars, M.; Roy, S. Hydrophobic Shape-Memory Biocomposites from Tung-Oil-Based Bioresin and Onion-Skin-Derived Nanocellulose Networks. *Polymers* **2020**, *12*, 2470. [\[CrossRef\]](#)
15. Balanuca, B.; Komartin, R.S.; Necolau, M.I.; Damian, C.M.; Stan, R. Investigating the Synthesis and Characteristics of UV-Cured Bio-Based Epoxy Vegetable Oil-Lignin Composites Mediated by Structure-Directing Agents. *Polymers* **2023**, *15*, 439. [\[CrossRef\]](#)
16. Biswas, E.; Silva, J.A.C.; Khan, M.; Quirino, R.L. Synthesis and Properties of Bio-Based Composites from Vegetable Oils and Starch. *Coatings* **2022**, *12*, 1119. [\[CrossRef\]](#)
17. Gogoi, G.; Chowdhury, C.; Maji, T.K. Effect of Nanoclay on the Properties of Rosin Derivative Cross-Linked Green Composite Based on Chicken Feather Fiber and Modified Vegetable Oil. *Polym. Eng. Sci.* **2021**, *61*, 288–300. [\[CrossRef\]](#)
18. Echeverri, D.A.; Inciarte, H.C.; Gómez, C.L.; Rios, L.A. Development of Glass Fiber/Unsaturated Polyester-like Resins Based on Modified Castor Oil. *Iran. Polym. J. Engl. Ed.* **2022**, *31*, 595–604. [\[CrossRef\]](#)
19. Tang, Q.; Li, Q.; Pan, X.; Xi, Z.; Zhao, L. Poly(Acrylated Epoxidized Soybean Oil)-Modified Carbon Nanotubes and Their Application in Epoxidized Soybean Oil-Based Thermoset Composites. *Polym. Compos.* **2021**, *42*, 5774–5788. [\[CrossRef\]](#)
20. Smith, M.; Payne, A.; Edwards, K.; Morris, S.; Beckler, B.; Quirino, R.L. Effect of Microwave Cure on the Thermo-Mechanical Properties of Tung Oil-Based/Carbon Nanotube Composites. *Coatings* **2015**, *5*, 557–575. [\[CrossRef\]](#)
21. Xu, Y.; Dai, S.; Zhang, H.; Bi, L.; Jiang, J.; Chen, Y. Reprocessable, Self-Adhesive, and Recyclable Carbon Fiber-Reinforced Composites Using a Catalyst-Free Self-Healing Bio-Based Vitrimers Matrix. *ACS Sustain. Chem. Eng.* **2021**, *9*, 16281–16290. [\[CrossRef\]](#)
22. Chen, B.; Liao, M.; Sun, J.; Shi, S. A Novel Biomass Polyurethane-Based Composite Coating with Superior Radiative Cooling, Anti-Corrosion and Recyclability for Surface Protection. *Prog. Org. Coat.* **2023**, *174*, 107250. [\[CrossRef\]](#)
23. Kim, K.M.; Kim, H.; Kim, H.J. Enhancing Thermo-Mechanical Properties of Epoxy Composites Using Fumed Silica with Different Surface Treatment. *Polymers* **2021**, *13*, 2691. [\[CrossRef\]](#)
24. Chen, W.; Wu, Z.; Xie, Y.; He, X.; Su, Y.; Qin, Y.; Tang, D.; Oh, S.K. Fabrication of Silane and Nano-Silica Composite Modified Bio-Based WPU and Its Interfacial Bonding Mechanism with Cementitious Materials. *Constr. Build. Mater.* **2023**, *371*, 130819. [\[CrossRef\]](#)
25. Alameri, I.; Oltulu, M. Mechanical Properties of Polymer Composites Reinforced by Silica-Based Materials of Various Sizes. *Appl. Nanosci.* **2020**, *10*, 4087–4102. [\[CrossRef\]](#)
26. Nartop, D.; Kazak, Ç. Synthesis and Characterization of Novel Polystyrene-Silica Composites Containing Azomethine. *J. Mol. Struct.* **2021**, *1227*, 129705. [\[CrossRef\]](#)
27. Slieptsova, I.; Savchenko, B.; Sova, N.; Slieptsov, A. Polymer Sand Composites Based on the Mixed and Heavily Contaminated Thermoplastic Waste. *IOP Conf. Ser. Mater. Sci. Eng.* **2016**, *111*, 012027. [\[CrossRef\]](#)
28. Zahran, R.R. Effect of Sand Addition on the Tensile Properties of Compression Moulded Sand/Polyethylene Composite System. *Mater. Lett.* **1998**, *34*, 161–167. [\[CrossRef\]](#)
29. Aston, J.E.; Wahlen, B.D.; Davis, R.W.; Siccardi, A.J.; Wendt, L.M. Application of Aqueous Alkaline Extraction to Remove Ash from Algae Harvested from an Algal Turf Scrubber. *Algal Res.* **2018**, *35*, 370–377. [\[CrossRef\]](#)
30. Kartik, A.; Akhil, D.; Lakshmi, D.; Panchamoorthy Gopinath, K.; Arun, J.; Sivaramakrishnan, R.; Pugazhendhi, A. A Critical Review on Production of Biopolymers from Algae Biomass and Their Applications. *Bioresour. Technol.* **2021**, *329*, 124868. [\[CrossRef\]](#)
31. Bohre, A.; Modak, A.; Chourasia, V.; Ram Jadhao, P.; Sharma, K.; Kishore Pant, K. Recent Advances in Supported Ionic Liquid Catalysts for Sustainable Biomass Valorisation to High-Value Chemicals and Fuels. *Chem. Eng. J.* **2022**, *450*, 138032. [\[CrossRef\]](#)
32. Di Mauro, C.; Genua, A.; Mija, A. Fully Bio-Based Reprocessable Thermosetting Resins Based on Epoxidized Vegetable Oils Cured with Itaconic Acid. *Ind. Crops Prod.* **2022**, *185*, 115116. [\[CrossRef\]](#)
33. Murawski, A.; Quirino, R.L. Bio-Based Composites With Enhanced Matrix-Reinforcement Interactions from the Polymerization of α -Eleostearic Acid. *Coatings* **2019**, *9*, 447. [\[CrossRef\]](#)
34. Johns, A.; Morris, S.; Edwards, K.; Quirino, R.L. Asolectin from Soybeans as a Natural Compatibilizer for Cellulose-Reinforced Biocomposites from Tung Oil. *J. Appl. Polym. Sci.* **2015**, *132*, 41833. [\[CrossRef\]](#)
35. Quirino, R.L.; Larock, R.C. Rice Hull Biocomposites, Part 2: Effect of the Resin Composition on the Properties of the Composite. *J. Appl. Polym. Sci.* **2011**, *121*, 2050–2059. [\[CrossRef\]](#)
36. Conti Silva, J.A.; Walton, H.; Dever, S.; Kardel, K.; Martins Lacerda, T.; Lopes Quirino, R. Itaconic Anhydride as a Green Compatibilizer in Composites Prepared by the Reinforcement of a Tung Oil-Based Thermosetting Resin with Miscanthus, Pine Wood, or Algae Biomass. *Coatings* **2023**, *13*, 25. [\[CrossRef\]](#)
37. Xiao, R.; Yang, W.; Cong, X.; Dong, K.; Xu, J.; Wang, D.; Yang, X. Thermogravimetric Analysis and Reaction Kinetics of Lignocellulosic Biomass Pyrolysis. *Energy* **2020**, *201*, 117537. [\[CrossRef\]](#)

38. Blivi, A.S.; Benhui, F.; Bai, J.; Kondo, D.; Bédoui, F. Experimental Evidence of Size Effect in Nano-Reinforced Polymers: Case of Silica Reinforced PMMA. *Polym. Test.* **2016**, *56*, 337–343. [[CrossRef](#)]
39. Silverstein, R.M.; Webster, F.X. *Spectrometric Identification of Organic Compounds*, 6th ed.; John Wiley & Sons: New York, NY, USA, 1998.

Disclaimer/Publisher’s Note: The statements, opinions and data contained in all publications are solely those of the individual author(s) and contributor(s) and not of MDPI and/or the editor(s). MDPI and/or the editor(s) disclaim responsibility for any injury to people or property resulting from any ideas, methods, instructions or products referred to in the content.